ACS OMEGA

http://pubs.acs.org/journal/acsodf

Article

Experimental Study on the Dynamic Tensile Characteristics of Coal Samples

Han Meng, Yuzhong Yang,* Liyun Wu, Daming Yang, and Chenlin Wang

Cite This: *ACS Omega* 2023, 8, 5506−5521

Read Online

ACCESS | Metrics & More | Article Recommendations

ABSTRACT: As coal mines continue deep mining, the frequency of coal and rock dynamic disasters has also gradually increased. In this paper, dynamic tensile strength deformation, energy evolution, and crack development under an impact test were studied on Brazilian coal samples, using a split Hopkinson pressure bar (SHPB) test device. A high-speed camera was adopted to capture the failure process of the coal specimens. The research results demonstrate that when the impact velocity is greater than 4.75 m/s, the dynamic tensile strength of the vertical bedding direction is higher than that of the parallel bedding direction of the coal samples. With the increase in the impact velocity, the dynamic strain and ultimate strain rate of two types of coal samples are increased, and the average value of the first and second dynamic deformation moduli of coal samples shows decreasing characteristics. As the incident energy increases, the sum of reflected and transmitted energy increases, and the absorbed energy also increases in the two types of coal samples. The two types of Brazilian disc coal samples mainly showed tensile and shear failure characteristics. The dynamic tensile deformation characteristics of the two types of coal specimens are less affected by the impact angles. However, the crack propagation of coal samples was mainly influenced by the impact angles. The test results can be used for the prediction of coal and rock outburst in deep underground coal excavation.

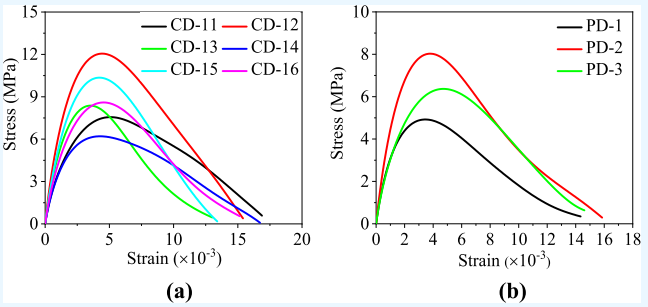

1. INTRODUCTION

With the continuous extension of coal mines to deep mining, the permeability of the coal seam is significantly reduced, the in situ stress and gas pressure are significantly increased, and the engineering conditions for deep coal mining become harsher.[1−4] The high-intensity mining operations by mining, drilling, and firing are always the inducing factors of dynamic disasters, which lead to increasing frequency of dynamic disasters, e.g., coal and gas outburst, rock burst, and mine earthquakes.[5−9] In detail, there will be no coal mining disasters if there are no human mining disturbances. Under the influence of mining activities, the original physical state equilibrium of coal rock will be broken, and then the typical dynamic disaster of coal rock will occur. Therefore, to prevent and predict coal rock dynamic disasters, it is very necessary to investigate the dynamic deformation and failure of the coal rock behaviors using dynamic mechanical methods. Split Hopkinson pressure bar (SHPB) experimental techniques were widely used to test the dynamic strength characteristics of plastic materials and brittle materials. In particular, SHPB technology was not only suitable for testing the dynamic strength characteristics of concrete materials, but also often used to test the dynamic strength parameter characteristics of rock materials.[10−13]

The SHPB system has been adopted substantially for the measurement of the dynamic failure characteristics of coal rock specimens.[14−20] Kumar and Hakalehto[21,22] first adopted the SHPB device to conduct dynamic compressive strength on basalt and granite. Klepaczko[23] et al. found that the fracture toughness of Canadian coal samples increases by one order of magnitude during dynamic impact than during quasi-static. Through the SHPB test techniques, some scholars found that the dynamic compressive strength and elastic moduli of the rocks are relatively high.[24,25] Chen et al.[26] provided a detailed summary of the entire process of SHPB rods from the device design, evaluation, and applications. In addition, Zhang et al.[27] reviewed and summarized the development of 50 years of dynamic experimental techniques and the dynamic mechanical behavior of rocks, and included related constitutive models.

Recently, some scholars have carried out experiments on the dynamic tensile characteristics of coal rock and studied the influence of different loading rates, loading angles, and the characteristics of the specimen itself in dynamic experiments. Some researchers developed dynamic tensile tests, such as the

Received: October 20, 2022
Accepted: December 30, 2022
Published: February 6, 2023

Brazilian disc, this method was widely used to measure the dynamic tensile parameters of coal rock specimens. The Brazilian disc follows a dynamic equilibrium process, and the equilibrium process is confirmed by numerical simulation methods.[28] From the perspective of the dynamic tensile properties in the experiment, the bedding direction is essential in dynamic mechanical features and the crack evolution of coal samples.[29] Zhao et al.[30,31] investigated and found that the impact velocity is proportional to the dynamic tensile strength, and the impact angle mainly affects the failure mode of the coal samples. Zhang et al.[32] using a high-speed camera and digital speckle technology in the SHPB test, analyzed the dynamic crack initiation toughness, tensile strength, and uniaxial compressive strength of Fangshan marble. Zhu et al.[33] using the SHPB system investigated the dynamic tensile properties of the coal samples. Based on this, they found that the strength of the water-retaining coal sample is lower, and saturated coal has less debris between 0 and 5 mm after crushing. Xia et al.[34] illustrated that the dynamic tensile strength of the coal and sandstone samples is 1.5 and 3 times their corresponding static tensile strength. Gong et al.[35] adopted a new empirical equation to analyze the indirect tensile strength of the sandstone under the dynamic impact experiment. Huang et al.[36] studied the characteristics of saturated and dry Longyou sandstone, and concluded that the softening coefficient and factor of the two types of samples decreased with the loading rate, but were more sensitive to the loading of the saturated coal samples.

However, the abovementioned scholars have not researched the energy change characteristics of the samples, when they carried out dynamic experiments on coal and rock samples. Most research relates to the test literature on the energy evolution of the rock dynamics. Lundberg[37] analysis of the characteristics of energy change of granite and limestone during the dynamic impact test, using the established stiffness plastic model, concluded that the samples absorb energy less than half of the incident energy during the dynamic test. Zhang et al.[38] studied the evolution of energy characteristics of the Fangshan gabbro and marble during dynamic shock experiments. Li et al.[39] found that under the dynamic impact experiment, the absorb energy of the specimens was positively correlated with the strain rate. The fragments formed after the specimen is fractured consume energy, and the size of the fragments is closely related to the energy absorption. From the summary of the essential characteristics of energy evolution of coal rock specimens under dynamic experiment, the specimens first absorb energy when it is impacted by an external force, and then begins to deform and destroy, that is the dissipation of energy. Moreover, there are some unclear laws of the dynamic tensile strength of coal samples. Thus, it is necessary to quantify the contribution of bedding structures on dynamic tensile strength and deformation of coal samples.

In this paper, further investigation of the dynamic tensile properties of vertical and parallel bedding coal samples was conducted by SHPB tests. We explores the relationship of the impact velocity and impact angle with the dynamic tensile strength, strain, and strain rate of coal samples. The energy evolution characteristics of vertical and parallel bedding coal samples under dynamic tensile experiments were analyzed. This paper also examines the fracture propagation characteristics of coal samples, as monitored by a high-speed camera system.

2. EXPERIMENTAL PROCEDURE

2.1. Coal Sample Preparation. The experimental coal samples were taken from the Ji_{15-17} 11110 mining face of 13 mines of Pingdingshan Tian'an Coal Industry Co., Ltd. The average mining depth of the comprehensive mining face is 591.6 m. The coal samples preparation standard followed the recommendation of the International Society for Rock Mechanics (ISRM), the size of the coal specimens was Ø 50 mm × h 25 mm.[40−42] The roughness of the two end face of the specimens was less than 0.05 mm. A total of 44 specimens were prepared for this test (Figure 1). The coal samples cored in the parallel layer direction were defined as the PD group, and the coal samples cored in the vertical direction were the CD group.

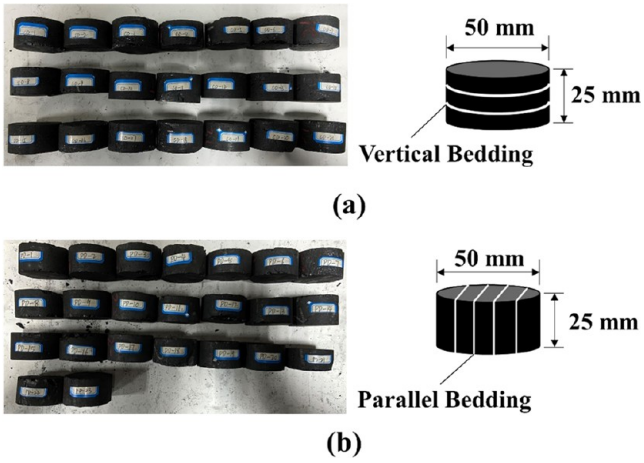

Figure 1. Coal samples prepared for dynamic impact experiments (a) vertical bedding coal samples and (b) parallel bedding coal samples.

When carrying out the dynamic tensile experiment, coal samples of the same specification with no obvious defects in appearance and relatively close wave speeds were selected. The basic parameters of the coal samples are as follows: moisture content of 1.11%; ash content of 9.14%; volatilization of 18.20%, and coal density of 1.4 t/m^3.

2.2. Split Hopkinson Pressure Bar System. This dynamic shock experiment was carried out on the SHPB experimental system of Henan Polytechnic University, and the system is shown in Figure 2. During the experiment, the impact speed of the bullet was controlled by adjusting the N_2 pressure in the gas pressure chamber and the position of the bullet in the firing chamber. Then, the dynamic impact experiments of coal samples under different impact velocities were realized.

In this SHPB experimental device, the length of the incident bar was 3000 mm and the diameter was 50 mm, the length of the transmission bar was 3000 mm and the diameter was 50 mm, the bullet length was 400 mm, the elastic modulus of the rod was 210 GPa, and the wave velocity of the elastic wave was 5172 m/s. The depth values of the striker were set to 600 mm and 800 mm.

2.3. Principle Analysis of SHPB. In this experiment, the direct impact test was carried out on the CD group coal samples; for the PD group coal samples, the impact test was carried out with impact angles of 0, 30, 60, and 90°, between the impact direction and bedding direction of the coal samples (Figure 2c). Meanwhile, a variety of means were used to carry out the quality control of the experiment. Before the formal

https://doi.org/10.1021/acsomega.2c06760
ACS Omega 2023, 8, 5506−5521

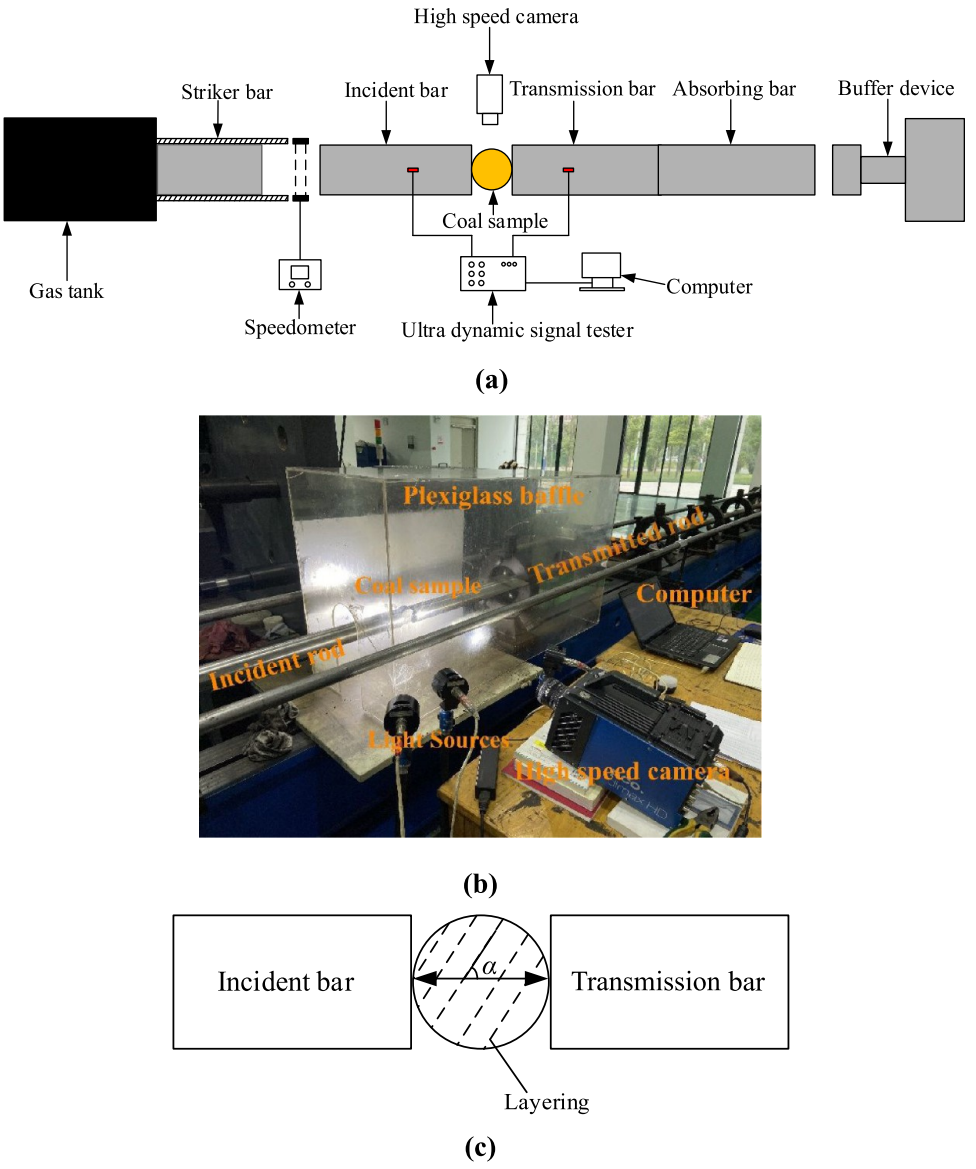

Figure 2. Configuration of the SHPB testing system (a) Experimental system layout drawing; (b) Photograph of the test equipment; (c) SHPB loading diagram.

experiment, a filter experiment should be performed with a paper card to filter out the high-frequency oscillation spikers that may appear in the waveform until a satisfactory sine wave is obtained. The filtering method is to first apply butter to the center of the end where the incident rod is in contact with the bullet and attach a round paper card with a diameter of 20 mm and a thickness of 0.3 mm. Subsequently, experiments are started and the corresponding bullet velocity is obtained at different bullet depths and gas pressures. In the placement of experimental specimens between the incident bar and transmitted bar, and the absorption bar and the buffer device are to be coated with grease, to reduce the end friction effect between the rods on the experimental results of adverse effects. Meanwhile, the manufacturer's data processing software is used to pre-process the experimental waveform, and the incident, reflected, and transmitted waves are then processed twice to ensure the accuracy and regularity of the experimental data. When a coal sample participating in the dynamic tensile test was completely broken, the data of the high-speed camera are saved manually, and then the broken coal samples were cleaned. Next, according to the experimental scheme and the above steps were repeated to start the next coal sample experiment.

In this paper, we adopted ISRM-suggested rules to carry out this experiment.[42] Based on the incident wave, reflected wave, and transmitted wave obtained by the shock experiment, the characteristics of coal samples under shock load were analyzed. Using three-dimensional stress wave theory, the expressions for the dynamic strain $\varepsilon(t)$, dynamic stress $\sigma(t)$, and dynamic strain rate $\dot{\varepsilon}$ of the coal sample were obtained.[43−45]

$$\varepsilon(t) = \frac{C_0}{l_s}\int_0^t [\varepsilon_I(t) - \varepsilon_R(t) - \varepsilon_T(t)]\mathrm{d}t \tag{1}$$

$$\dot{\varepsilon} = \frac{C_0}{l_s}[\varepsilon_I(t) - \varepsilon_R(t) - \varepsilon_T(t)] \tag{2}$$

$$\sigma(t) = \frac{A_0 E_b}{2A_s}[\varepsilon_I(t) + \varepsilon_R(t) + \varepsilon_T(t)] \tag{3}$$

https://doi.org/10.1021/acsomega.2c06760
ACS Omega 2023, 8, 5506−5521

Table 1. Dynamic Tensile Test Results of CD Group Coal Samples

no.	impact velocity v (m/s)	dynamic tensile strength (MPa)	extreme strain ε_m($\times10^{-3}$)	peak strain ε_p($\times10^{-3}$)	strain rate $\dot{\varepsilon}$(s^{-1})	the first dynamic modulus of elasticity (GPa)	the second dynamic modulus of elasticity (GPa)	destroy time T_D (μs)
CD-1	3.695	3.99	8.95	2.15	68.95	3.88	1.22	167.5
CD-2	3.732	8.61	9.81	2.85	46.41	6.52	1.97	268.0
CD-3	3.242	5.06	10.09	3.06	52.87	3.61	1.07	265.0
CD-5	3.415	8.45	10.20	3.16	61.56	6.04	1.72	201.0
CD-6	3.427	8.64	10.82	2.51	58.82	8.15	2.18	256.0
CD-7	3.445	9.83	9.88	2.78	51.24	6.92	2.37	247.0
CD-8	3.973	3.27	13.85	2.65	71.70	2.68	0.80	260.0
CD-9	3.836	4.78	10.68	2.13	46.59	6.29	1.37	332.0
CD-10	3.979	11.42	11.80	2.66	70.43	9.06	2.81	208.0
CD-11	4.751	7.56	16.88	5.09	96.43	3.41	0.95	224.0
CD-12	5.25	12.05	15.40	4.45	81.26	6.09	1.74	253.0
CD-13	4.903	8.37	13.01	3.51	98.55	5.10	1.56	159.0
CD-14	5.254	6.20	16.73	4.27	103.10	3.60	0.91	196.0
CD-15	5.129	10.35	13.40	4.24	84.06	5.18	1.60	198.0
CD-16	5.023	8.60	15.16	4.56	99.64	4.17	1.22	181.0

Table 2. Dynamic Tensile Test Results of PD Group Coal Samples

no.	impact angle (deg)	impact velocity v (m/s)	dynamic tensile strength (MPa)	extreme strain ε_m ($\times10^{-3}$)	peak strain ε_p($\times10^{-3}$)	strain rate $\dot{\varepsilon}$ (s^{-1})	the first dynamic modulus of elasticity (GPa)	the second dynamic modulus of elasticity (GPa)	destroy time T_D (μs)
PD-1		5.104	4.92	14.34	3.46	95.61	3.46	0.89	172.5
PD-2		5.228	8.03	15.85	3.78	97.81	4.61	1.38	193.0
PD-3		5.15	6.37	14.61	4.72	71.51	2.95	0.88	271.5
PD-4	90	3.55	4.46	11.22	3.88	62.79	2.86	0.72	246.5
PD-5	90	3.42	11.96	9.2	3.21	66.80	8.19	2.41	175.0
PD-6	90	3.54	8.17	11.42	3.73	76.48	5.11	1.39	189.0
PD-7	90	3.524	4.58	12.95	3.70	76.02	2.69	0.80	283.0
PD-8	90	3.532	9.84	11.44	3.01	65.98	7.23	2.11	241.5
PD-9	0	3.922	1.66	13.16	2.77	79.90	1.43	0.38	199.5
PD-10	0	3.64	6.92	11.49	2.71	72.32	5.77	1.64	192.0
PD-11	0	4.099	1.09	15.37	9.35	86.07	0.36	0.07	247.0
PD-12	0	4.149	8.54	10.31	3.70	84.30	5.41	1.47	149.0
PD-13	0	4.021	7.65	11.17	3.49	63.05	4.78	1.42	233.5
PD-14	60	4.037	5.34	9.65	1.98	72.45	5.93	1.75	176.5
PD-15	60	3.836	7.55	12.79	3.12	76.50	5.39	1.56	205.5
PD-16	60	3.888	3.10	10.47	2.62	75.99	2.0	0.84	175.5
PD-17	60	4.291	7.05	13.48	3.69	89.95	4.58	1.21	174.0
PD-18	60	3.949	8.02	11.14	2.9	66.36	5.99	1.80	196.5
PD-19	30	3.969	6.34	11.25	2.99	61.76	4.40	1.40	220.0
PD-20	30	3.825	7.85	10.69	2.58	69.26	7.01	1.94	190.0
PD-21	30	3.711	9.66	10.19	2.5	51.45	8.33	2.52	237.0
PD-23	30	3.896	4.3	9.34	3.13	47.51	2.99	0.89	244.0

where C_0 is the elastic wave velocity of the rod, m/s; A_0 is the cross-sectional area of the rod, mm^2; E_b is the modulus of elasticity of the pressure rod, GPa; l_s is the initial cross-sectional area of the specimen, mm^2; A_s is the initial length of the specimen, mm; $\varepsilon_I(t)$ is the incident strain of the compression rod; $\varepsilon_R(t)$ is the strain of the compression rod; and $\varepsilon_T(t)$ is the transmission strain of the rod. In this paper, the strain of the rod is uniformly defined as a positive value.

3. RESULTS

3.1. Characteristics of Stress−Strain Curves. According to eqs 1−3, the characteristic parameters of the vertical seam group (CD group) and parallel seam group coal samples (PD group) after the dynamic tensile tests were sorted and analyzed, and the dynamic tensile test results are shown in Tables 1 and 2. In this paper, we believe that the crushing of the coal sample occurred when it is destroyed, so the dynamic peak stress in the stress−strain curve is the dynamic tensile strength of the coal samples.

The stress−strain curves of the dynamic tensile test of the coal samples in the CD group and PD group is shown in Figure 3. In the dynamic tensile impact experiment on the PD group coal samples, when the impact angles were 0, 30, 60, and 90°, we used the same velocity, and the average velocity is 3.83 m/s. From the stress−strain curve analysis of the two groups of coal samples, it was found that the distribution of the tensile strength parameters of the coal samples has certain discrete characteristics due to the heterogeneity of the coal samples.

As shown in Figure 3, the dynamic stress−strain curves of coal samples can be divided into four stages, the first stage is an approximately straight stage, the second stage is the nonlinear

https://doi.org/10.1021/acsomega.2c06760
ACS Omega 2023, 8, 5506−5521

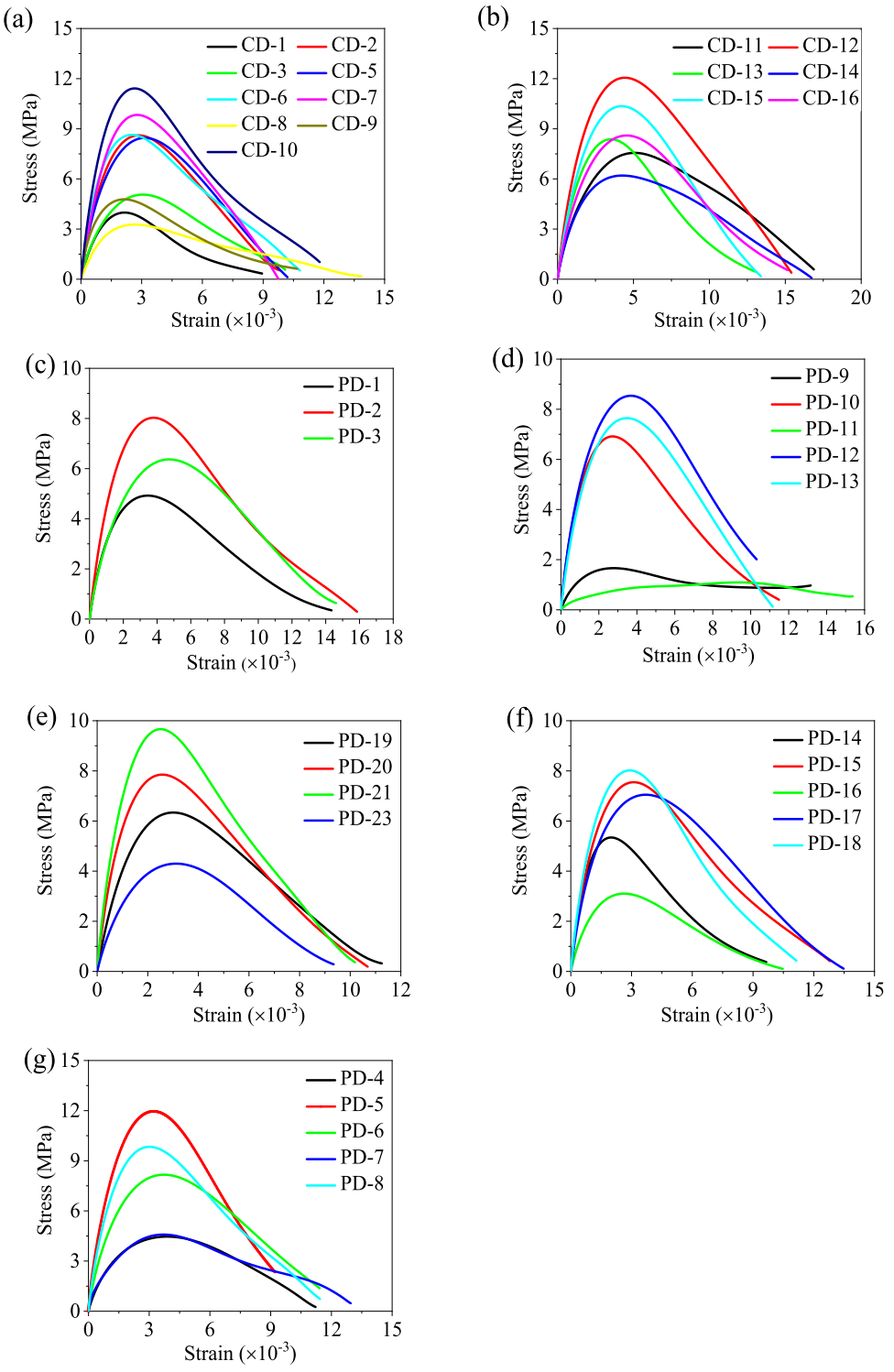

Figure 3. Dynamic stress−strain curves of CD and PD group coal samples (a) $\overline{v}$ = 3.64 m/s; (b) $\overline{v}$ = 5.05 m/s; (c) $\overline{v}$ = 5.16 m/s; (d) $\overline{v}$ = 5.16 m/s; (e) (d) w = 0°; (e) w = 30°; (f) w = 60°; and (g) w = 90°.

convex stage, the third stage is the approximate platform stage, and the fourth stage is the stress drop stage. This time, we take the coal sample CD-2 as an example to analyze the detailed stress and strain process of the coal samples.

Figure 4 exhibits the four damage level stages of the CD-2 coal sample, under the dynamic tensile experiment. The first stage is approximately a straight stage (OA stage). The curve characteristics of the stress−strain in the OA stage are similar to those of a straight line, and the slope in this phase is also relatively large. The reason is that under the action of dynamic impact, in which the microcracks and defects inside the material are not compacted to produce direct elastic deformation, that is, without the compaction stage of the coal sample under static loading. The nonlinear convex stage is the AB stage, in which the coal sample produces a certain plastic deformation as the impact of the load continues to

https://doi.org/10.1021/acsomega.2c06760
ACS Omega 2023, 8, 5506−5521

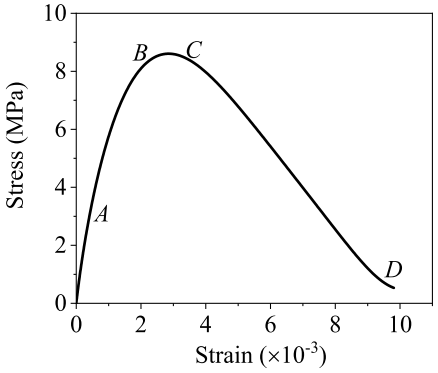

Figure 4. Dynamic stress−strain curves of the CD-2 coal sample.

increase. Meanwhile, the dynamic stress−strain curves of the coal sample show a certain nonlinear relationship. Secondary cracks and failures have formed within the coal sample, but no new macroscopic fracture surfaces have emerged. In general, the stress−strain curve shows a nonlinear upward trend and characteristics. The BC stage is a similar platform stage, the stress−strain curve presents the characteristics of an approximate platform, and the coal has been broken, but the crushed block has not completely separated from the whole samples. The friction between the fragments continues to maintain the residual strength of the coal sample, so the stress−strain curve presents a transient stress yield plateau. The stress fall stage is the CD stage, in which a macroscopic fracture surface inside the coal sample has gradually been generated. And then the coal sample has also been completely broken at this time, and the crushing ability to resist impact has gradually decreased. Consequently, the stress−strain curve has shown a certain drop characteristic.

Figure 5 shows the specific relationship between the peak stress and the impact velocity during the dynamic tensile test

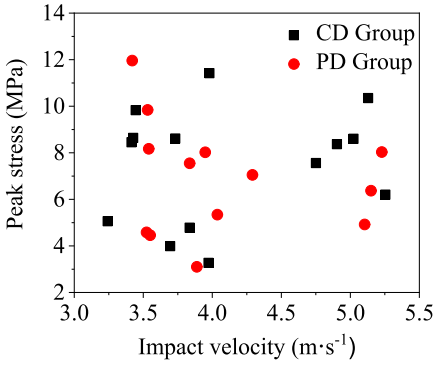

Figure 5. Relationship between impact velocity and peak strength of coal samples.

of the coal samples. When the impact velocity is less than 4.75 m/s, the impact velocity has little effect on the peak stress of the CD group and PD group coal samples, and the numerical value difference in the dynamic tensile strength of the two groups of coal samples is very small.

However, when the impact velocity is greater than 4.75 m/s, the peak stress of the dynamic tensile resistance of the two groups of coal samples gradually increases. When the impact velocity was kept constant, the dynamic tensile strength values were characterized by CD group > PD group coal samples. This can be explained by that the bedding direction has a great influence on the dynamic mechanical properties of the coal samples. The CD group sample was cored in the vertical laminal direction, while the compactness is relatively high. The PD group coal samples were cored in the parallel direction, and the internal fissures of the coal samples were relatively developed. Meanwhile, when the impact velocity was less than 4.75 m/s, the failure of the coal sample was not complete, resulting in the nonobvious relationship between the dynamic tensile strength and impact velocity.

3.2. Deformation Characteristics of Coal Samples.

3.2.1. Characteristics of Dynamic Tensile Strain Rate of Coal Samples. The relationship between the strain rate and time dynamic tensile tests of coal samples in CD and PD groups is shown in Figure 6. Where, $\overline{v}$ is the average impact velocity, m/s; w is the direction of the shock load applied, and own bedding angle of coal samples, °.

Figure 6 exhibits that there will be a more obvious yield platform near the peak strain rate because the stress waves generated by the SHPB test system are rectangular waves. Moreover, when the external load reaches the impact resistance of the coal samples, due to the short impact time, the coal samples will have an adaptation stagnation period after crushing. Hence, a continuous strain rate is characterized by a short period. The two groups of coal samples have certain similar characteristics in the strain rate and time curve, and a plateau stage of a certain width will appear near the peak strain rate. The reason is that this dynamic impact test uses a cylindrical bullet, and the stress wave generated is a rectangular wave. However, the external force of the impact is relatively short when it reaches the maximum impact capacity that the coal samples can withstand. Although the coal samples has been damaged, it can continue to bear external stress by relying on the friction between particles.

The characteristic relationship between the max strain rate and impact velocity during the dynamic tensile resistance of the two groups of coal samples is shown in Figure 7. With the increase of the impact speed, the strain rate of the coal samples also gradually increases. Moreover, the impact speed has a greater effect on the strain rate than the different bedding directions of coal samples. Overall, the effect of the impact on the strain rate of the coal samples is the most obvious.

The experimental data of the coal samples max strain rate and impact velocity are fitted, and the fitting relationship of coal samples in the CD group is shown in eq 4. The fitting relationship between the impact velocity and the dynamic max strain rate of the coal samples in the PD group is shown in eq 5.

$$y = 23.13x - 24.46 \quad R^2 = 0.75 \tag{4}$$

$$y = 13.61x + 17.98 \quad R^2 = 0.57 \tag{5}$$

From the perspective of the relationship characteristics of fitting, the fitting value of the impact velocity and strain rate of the coal sample in the CD group was 0.75, and the fitting value of the coal sample in the PD group was 0.57. This indicates that in the tensile impact test of coal samples in the CD group, the strain rate of coal samples has a close relationship with impact velocity, showing a good linear relationship. However, the fitting relationship between strain rate and impact velocity of coal samples in the PD group was poor. In eq 5, it was found that the dynamic strain rate has a positive correlation with the impact velocity of PD group coal samples. In general, the strain rate of coal samples was closely related to the structure of coal

https://doi.org/10.1021/acsomega.2c06760
ACS Omega 2023, 8, 5506−5521

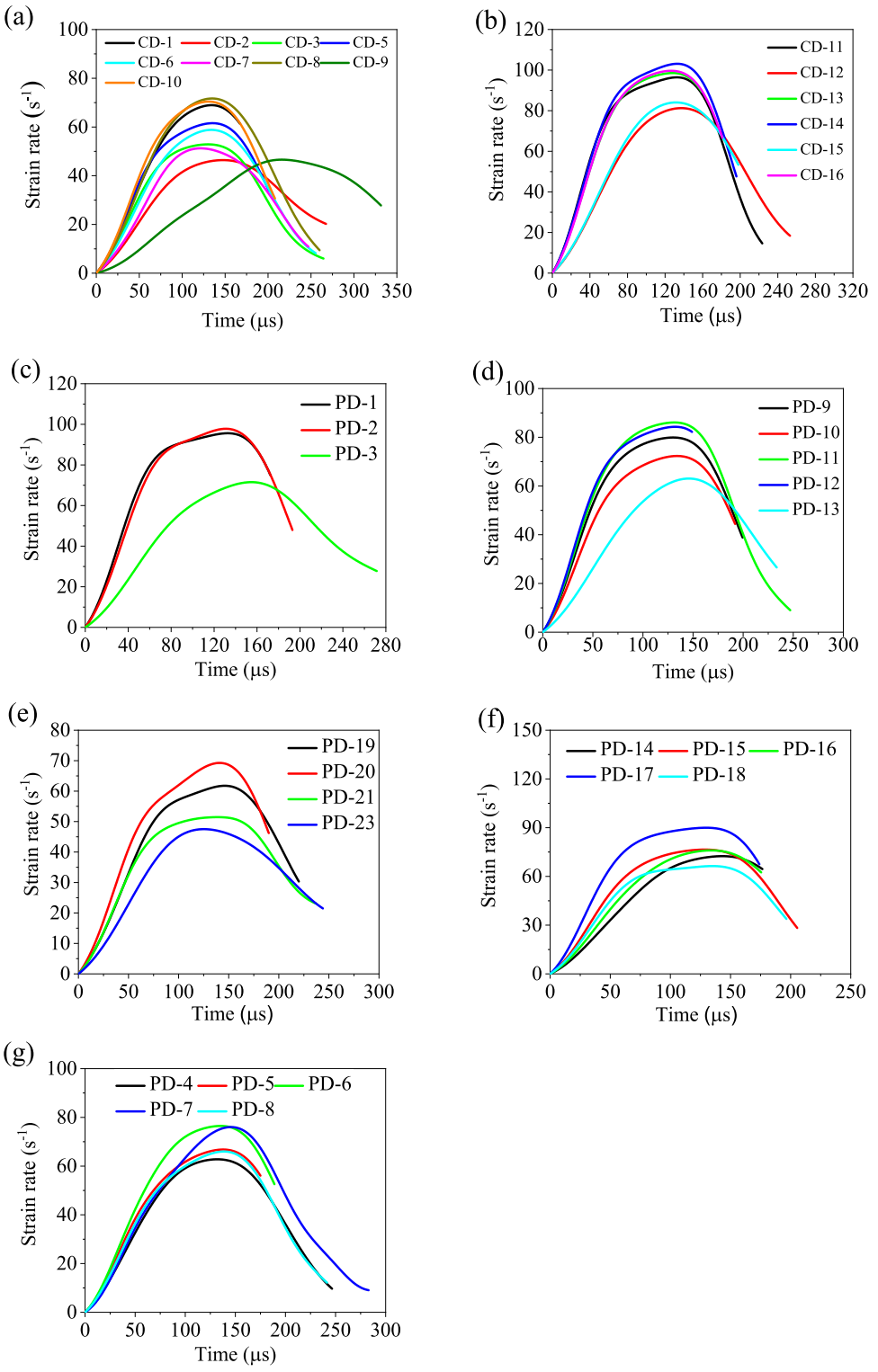

Figure 6. Relationship between the dynamic strain rate and time in the tensile test of the coal sample (a) $\overline{v}$ = 3.64 m/s; (b) $\overline{v}$ = 5.05 m/s; (c) $\overline{v}$ = 5.16 m/s; (d) w = 0°; (e) w = 30°; (f) w = 60°; and (g) w = 90°.

samples during dynamic tensile impact experiments. Therefore, the strain rate change characteristics of vertical seamare more obvious than parallel seam of coal samples.

3.2.2. Characteristics of Ultimate Strain of Coal Samples. The ultimate strain and dynamic deformation moduli of the coal samples were used to characterize the dynamic tensile deformation characteristics of coal samples. The relationship between the ultimate strain and the impact velocity of the CD and PD group coal samples is shown in Figure 8. The limit strain of the two groups of coal samples increases with the increase of the impact velocity (Figure 8). In Tables 1 and 2, the tensile limit strain and impact velocity of the coal samples are summarized, we can find that the power function and one-

https://doi.org/10.1021/acsomega.2c06760
ACS Omega 2023, 8, 5506−5521

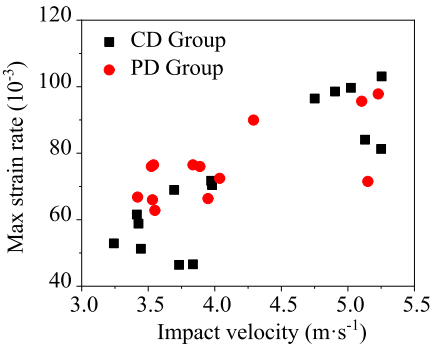

Figure 7. Relationship between the impact velocity and max strain rate of coal samples.

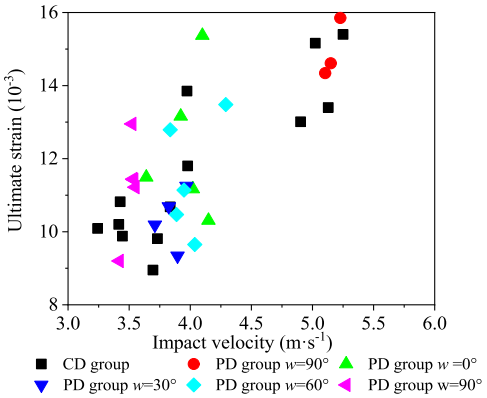

Figure 8. Ultimate strain characteristics of coal samples at different impact velocities.

time function are used to fit the relationship between the CD and, and the fitting result is shown in eqs 6 and 7.

$$y = 2.84x^{1.03} \quad R^2 = 0.75 \tag{6}$$

$$y = 2.38x + 2.49 \quad R^2 = 0.62 \tag{7}$$

Figure 8 shows that the dynamic tensile limit strain value of the two types of coal samples increases with the increase of the impact velocity. At an average impact velocity of 3.6 m/s, the average limit strain value of the PD group is greater than that of the CD group coal sample. However, when the average impact velocity was 5.20 m/s, the average ultimate strain values of the CD group and PD group coal samples were 1.51×10^{-2} and 1.49×10^{-2}. It was found that the two groups coal sample of the average ultimate strain were relatively close. However, from the analysis of the influencing characteristics of different impact angles on the ultimate strain values of the PD group, it can be found that under the same impact velocity, the average ultimate strain of the PD group coal samples was less affected by the impact angle.

Therefore, in the dynamic tensile experiment of coal samples, with the increase of impact velocity, the ultimate strain of CD group coal samples also shows the characteristics of linear increases.

3.2.3. Characteristics of Deformation Modulus of Coal Samples. The deformation characteristics of the coal samples dynamic experiment are different from those under conventional static mechanics experiments. Based on the research of relevant scholars, two dynamic deformation moduli of coal samples were defined by taking 50% of the peak strength of coal samples as the cut-off point. The first dynamic deformation modulus ($E_{0.5}{}^1$) and the second dynamic deformation modulus ($E_{0.5}{}^2$), and the expressions for the two deformation moduli are as follows[46,47]

$$E_{0.5}^1 = \frac{\sigma_{0.5}}{\varepsilon_{0.5}} \tag{8}$$

$$E_{0.5}^2 = \frac{\sigma_p - \sigma_{0.5}}{\varepsilon_p - \varepsilon_{0.5}} \tag{9}$$

where $\sigma_{0.5}$ is the peak stress, MPa; $\varepsilon_{0.5}$ is the strain value corresponding to 50% of the peak stress.

The variation characteristics of the dynamic deformation modulus with the impact velocity of the coal sample are shown in Figure 9a,b. At different impact velocities, the distribution of the first and second dynamic deformation moduli of the CD and PD group coal samples was relatively discrete.

Judging from the average values of the first and second dynamic deformation moduli of the PD group and CD group coal samples, the average value of the first and second moduli of the coal samples decreases with the increase of the impact velocity. Meanwhile, the average value of the two types of deformation moduli of the CD group is greater than the average value of the PD group coal sample. We difine the specific meanings of the two kinds of dyanmic deformation moduli under this experiment. The first dynamic deformation

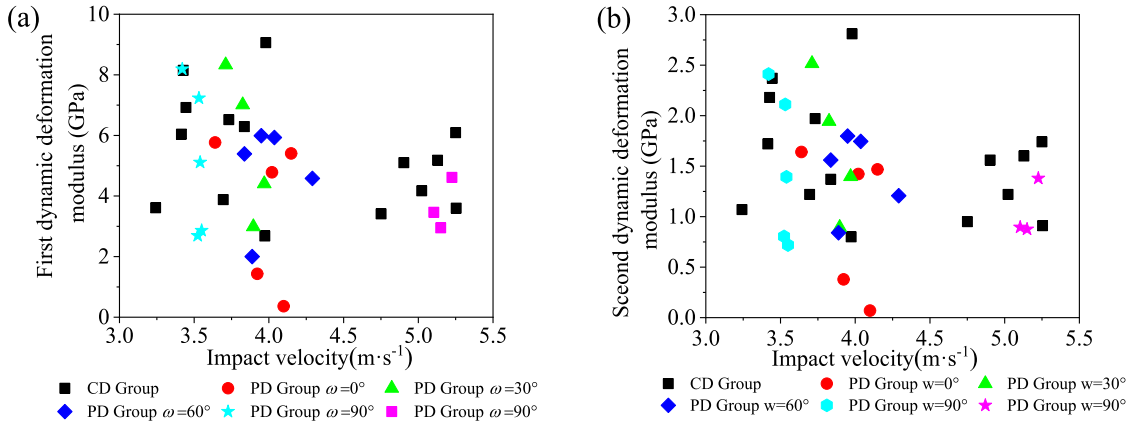

Figure 9. Variation rules of dynamic deformation modulus of coal samples in the tensile experiment. (a) First dynamic deformation modulus and (b) the second dynamic deformation modulus.

https://doi.org/10.1021/acsomega.2c06760
ACS Omega 2023, 8, 5506−5521

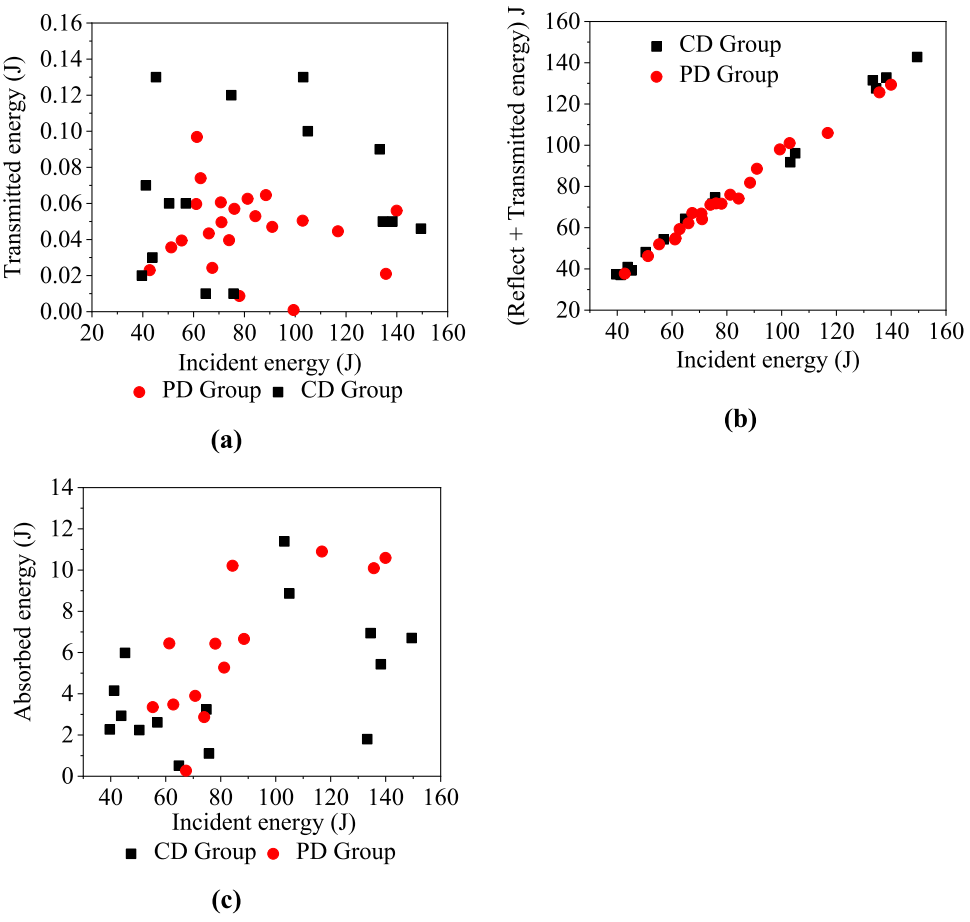

Figure 10. Energy variation characteristics of coal samples (a) Incident energy vs transmitted energy; (b) incident energy vs sum of reflected and transmitted energy; and (c) incident vs absorb energy.

modulus of the coal sample is more inclined to represent the deformation characteristics of the coal sample in the elastic stage, while the second dynamic deformation modulus is more inclined to represent the deformation characteristics of the coal sample in the plastic stage.

4. ENERGY EVOLUTION AND FAILURE CHARACTERISTICS OF COAL SAMPLES

4.1. Dynamic Tensile Energy Dissipation of Coal Samples. In this dynamic impact experiment of coal samples, from the application of dynamic load to the end of the experiment, the energy change of incident wave, reflected wave, and transmitted wave can be calculated and analyzed by the following equations.[48−50]

$$\left.\begin{aligned} W_{\mathrm{I}} &= \frac{A_0 C_{\mathrm{b}}}{E_{\mathrm{b}}} \int \sigma_{\mathrm{I}}^2(t)\mathrm{d}t \\ W_{\mathrm{R}} &= \frac{A_0 C_{\mathrm{b}}}{E_b} \int \sigma_{\mathrm{R}}^2(t)\mathrm{d}t \\ W_{\mathrm{T}} &= \frac{A_0 C_{\mathrm{b}}}{E_{\mathrm{b}}} \int \sigma_{\mathrm{T}}^2(t)\mathrm{d}t \end{aligned}\right\} \quad (10)$$

where W_{I} is the incident energy, J; W_{R} is the reflected energy, J; W_{T} is the transmitted energy, J; σ_{I} is the stress of the incident wave, kN; σ_{R} is the stress of the reflected wave, kN; and σ_{T} is the stress of the transmitted wave, kN.

When the dynamic impact test was performed on the coal samples, the contact area was relatively small because the contact between the coal samples and the pressure rod can be regarded as a linear contact. Meanwhile, smearing with butter was done to lubricate the contact surface between the coal samples and the pressure rod. Therefore, the energy generated by the friction between the coal samples and the pressure rod contact surface was not considered. In addition, the energy consumed in various forms such as thermal energy, radiation energy, and AE in the dynamic impact process was ignored, and the absorb energy and dissipate energy of the rock was considered equal in value. In this experiment, when analyzing the dynamic impact experimental data of those coal samples, clarification of the principle was necessary, that is, the coal samples must adsorb energy first, and then destruction will start to occur. Therefore, the dissipate energy W_d of the coal samples can be calculated according to energy conservation theory, as shown in the following equation

$$W_{\mathrm{d}} = W_{\mathrm{I}} - W_{\mathrm{R}} - W_{\mathrm{T}} \quad (11)$$

In eq 11, W_{d} is the dissipate energy of the coal sample, J.

According to the research results of the relevant scholars, the definition of the damage variable d of coal rock mass specimens during dynamic tensile failure in this paper is shown in eq 12.[51]

$$d = w_{\mathrm{d}}/u \quad (12)$$

https://doi.org/10.1021/acsomega.2c06760
ACS Omega 2023, 8, 5506−5521

where w_d is the total dissipate energy density of the coal sample, as shown in eq 13.

$$w_d = W_d/V \tag{13}$$

where V is the volume of the coal sample, mm^3.

where u is the total absorb energy density of the coal rock at the time of failure, which can be calculated by the area enclosed by the stress−strain curve of the coal sample under dynamic impact, as shown in eq 14.

$$u = \int \sigma \, d\varepsilon \tag{14}$$

Equations 10 and 11 were adopted to calculate the characteristic parameters of energy dissipation of coal samples in CD and PD groups. Meanwhile, the energy relationship analysis of the coal samples in CD and PD groups was carried out.

The relationship between the energy evolution characteristic in the dynamic tensile test of the two types of coal samples is shown in Figure 10.

Figure 10a shows that before the incident energy is below 88 J, the transmitted energy gradually increases in the PD group coal samples; after the incident energy is greater than 88 J, the transmitted energy will gradually show decreased characteristics of the PD group. Similarly, as far as the CD group is concerned, when the incident energy is larger than 103 J, the transmission energy also shows decreased characteristics.

Figure 10b shows with the increase in the incident energy, the sum of the reflected and transmitted energy of the two groups of coal samples will continue to increase. When the energy of the incident energy is increased to a certain value, the amplitude of the absorb energy of the coal sample will be further increased (Figure 10c). Then, after the incident energy reached 140 J, the amplitude of the absorb energy increase of the PD group coal sample will tend to be stable, while the absorb energy of the CD group coal sample is relatively discrete.

The relationship between the impact velocity and damage variable of the CD and PD group coal samples is shown in Figure 11. With the increase in the impact velocity, there was no obvious linear relationship between the damage variable and the impact velocity of coal samples in the CD group. Figure 11 shows that as the angle between the impact direction and the coal sample increases from 0 to 60°, the damage variable gradually increases for the PD group coal samples.

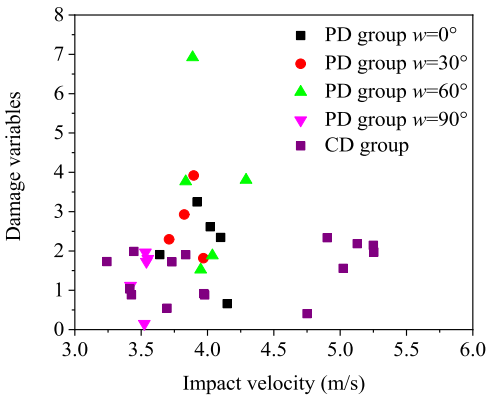

Figure 11. Relationship between the impact velocity and coal sample damage variables.

However, when the impact angle is 90°, the damage variable value of the PD group coal samples is the smallest. The reason is that when the impact direction is perpendicular to the layering direction of the PD group coal samples, the tensile strength value of the coal samples is the largest.

4.2. Failure Patterns of Coal Samples. The failure characteristics of the coal samples under dynamic impact are recorded by high-speed cameras, and then the dynamic tensile failure process of coal samples was analyzed. The dynamic tensile failure characteristics of CD group coal samples at different impact velocities are shown in Figures 12 and 13.

Figure 12 shows that the failure of the CD group coal samples is characterized by tensile failure along the diameter direction of the coal sample parallel to the impact direction of the coal sample. Furthermore, the shear failure band also appeared in the CD group coal samples because there were a certain number of cracks in the CD group coal samples, resulting in stress concentration near the weak surface of the coal sample under high strain rate conditions. Since the CD group coal samples is a vertically laminated core coal samples, only the impact velocity on the damage characteristics of the coal samples is considered during the loading process of the coal samples.

The failure mode of the dynamic tensile strength of CD group coal samples is shown in Figure 13. Tensile failure is the main cause of coal samples destruction, and there is a shear failure at the fracture development location of coal samples. The dynamic tensile failure characteristics of the CD group coal samples are more obvious with the increase in the impact velocity. With the increase of the impact velocity, the fragmentation characteristics of the coal samples are gradually enhanced, the fractal dimension is also increasing, and those of the coal samples with small particles gradually increase. The reason for the above phenomenon can be explained that as the impact velocity increases, the incident energy also becomes larger. Therefore, more energy is released when destruction occurs, increasing the degree of crushing of the coal samples.

The crack propagation characteristics of the PD group coal samples when the impact direction and bedding are at different angles are shown in Figure 14. The failure morphology of the PD group coal samples after the experiment is shown in Figure 15. It can be observed that, the PD group coal samples are mainly developed in the form of tensile failure. When the angle of impact is 0 and 90° in the laminar direction, the coal sample will expand along two straight cracks, and there will be a certain thickness of sheet coal samples between the two cracks (Figure 14). This indicates that the compactness of the coal sample itself is relatively good.

When the angle between the impact direction and the coal sample is 0 and 90°(Figure 14a,d), the impact failure characteristics of the two coal samples are very similar. However, when there is a relatively large crack in the coal sample, it will be destroyed along the weak surface formed by the fissure. This can be explained by the concentration of stress at the weak surface and then shear failure.

Judging from the damage characteristics of the PD group coal samples, the damage to the coal samples is less affected by the angle between the impact direction and the coal sample layer theory, and the impact rate is not large. In the process of impact failure, the dynamic tensile strength of the PD group coal samples was greatly affected by the internal fracture development and weak surface characteristics of the coal samples.

https://doi.org/10.1021/acsomega.2c06760
ACS Omega 2023, 8, 5506−5521

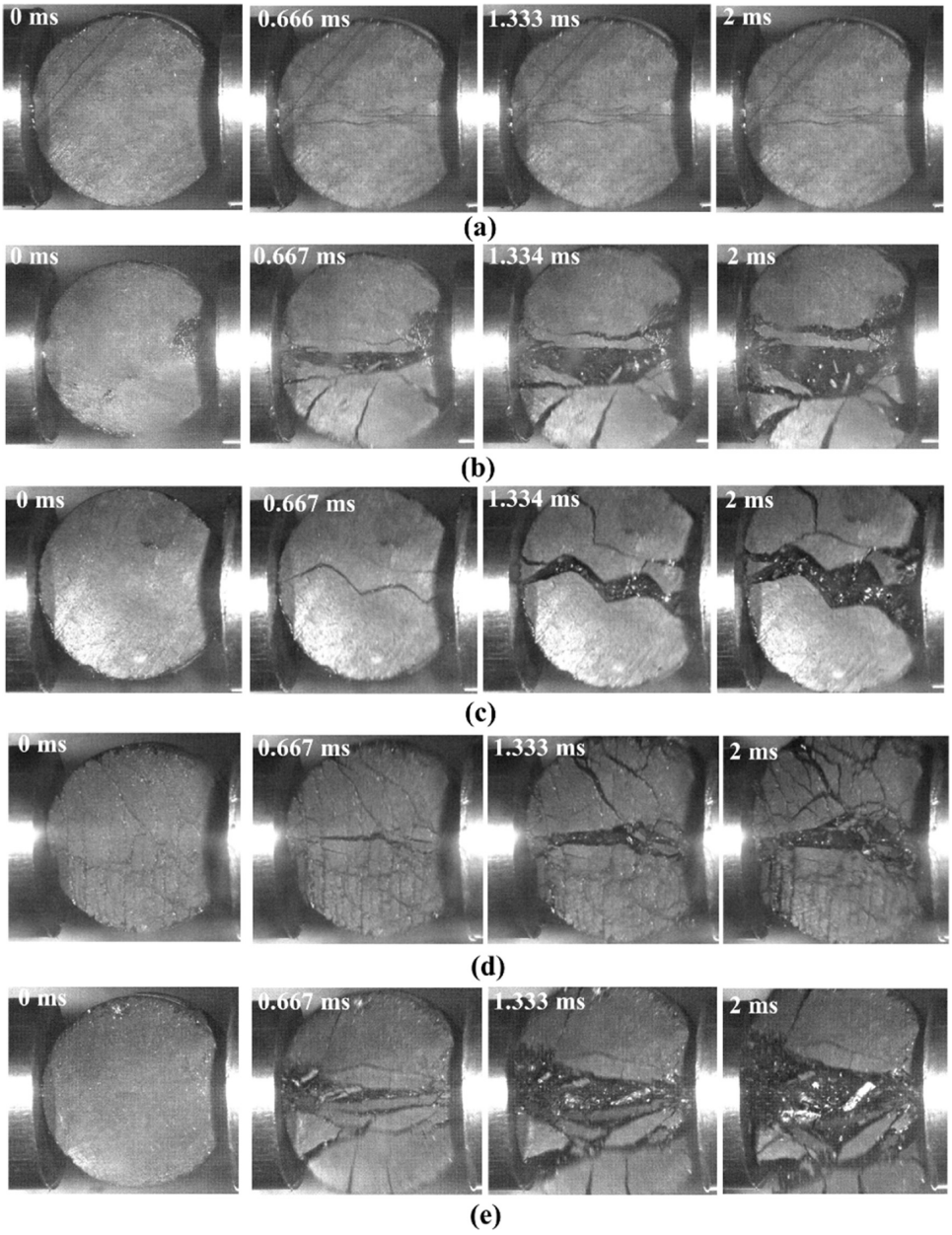

Figure 12. Failure process of the dynamic tensile strength of the CD group coal samples (a) CD-7, impact velocity = 3.445 m/s; (b) CD-2, impact velocity = 3.732 m/s; (c) CD-10, impact velocity = 3.979 m/s; (d) CD-16, velocity = 5.023 m/s; and (e) CD-15, velocity = 5.129 m/s.

5. DISCUSSION

5.1. Comparison of Dynamic Tensile Mechanical Parameters. From the stress−strain curve characteristics of the dynamic tensile of the coal samples, it was found that the dynamic tensile strength characteristics of the CD group coal samples are different although under the same impact velocity (Figure 3). For example, when the average impact velocity is 3.64 m/s, the average dynamic tensile strength of the CD-1, CD-3, CD-8, and CD-9 coal samples is 4.28 MPa, and the average dynamic tensile strength of the CD-2, CD-5, CD-6, CD-7, and CD-10 coal samples is 9.39 MPa. This shows that the average tensile strength of the CD group coal samples increases by 5.12 MPa under the same impact velocity conditions. Meanwhile, the dynamic failure time of the CD group coal samples decreased from 256.13 to 236 ms. It was also observed that the greater dynamic tensile strength of the coal samples, the smaller dynamic failure time of the coal samples; On the other hand, the brittleness characteristics of the latter group of coal samples are more obvious. However, from the dynamic strain rate data of the above two groups of coal samples, we can find that the difference between the average values is very small. From the analysis of the various characteristics of the CD group under the same impact velocity, we considered that it was affected by the strong heterogeneity of the coal samples. The physical and mechanical characteristics of coal samples are directly related to the coal structures. Coal is formed from the remains of plants through a variety of extremely complex physicochemical and geochemical cations, and the pore structure of coal determines the adsorption, permeability, and strength characteristics of the coal.[52]

When the average impact velocity increased to 5.05 m/s, the CD group coal samples value increase of peak strength,

https://doi.org/10.1021/acsomega.2c06760
ACS Omega 2023, 8, 5506−5521

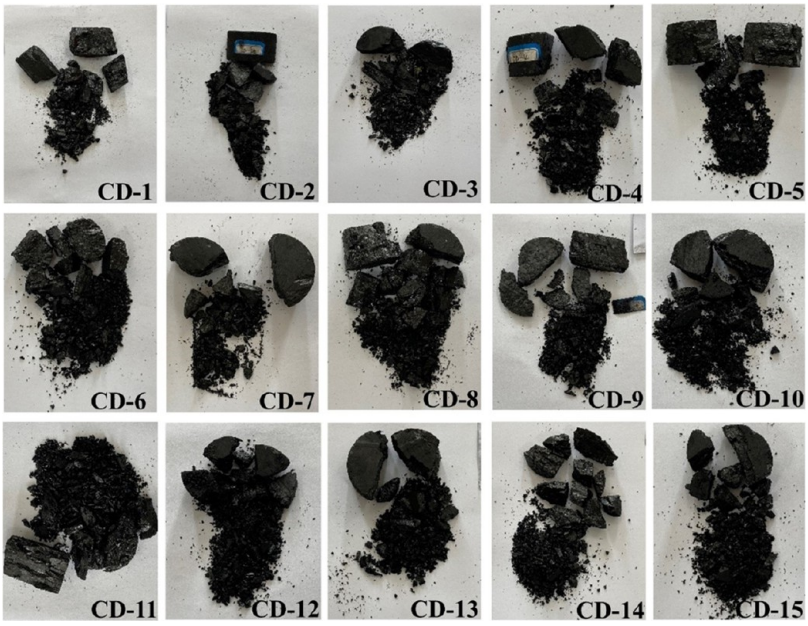

Figure 13. Dynamic tensile failure form of CD group coal samples.

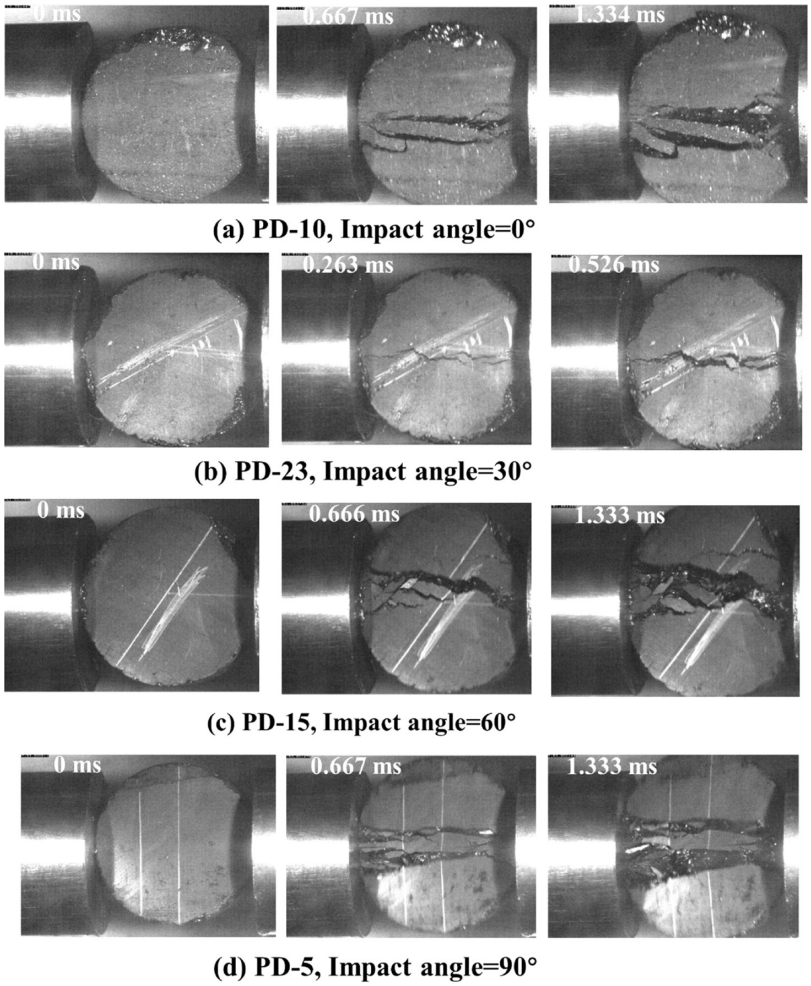

Figure 14. Dynamics tensile test of the PD group coal sample failure process under different impact angles (a) PD-10, impact angle = 0°; (b) PD-23, impact angle = 30°; (c) PD-15, impact angle = 60°; and (d) PD-5, impact angle = 90°.

extreme strain, peak strain, and strain rate were 29.60, 41.13, 64.6, and 59.43%, respectively. In contrast, the dynamic average impact time decreased by 44.23 s. It was observed that that the larger the impact velocity, the more obvious the

https://doi.org/10.1021/acsomega.2c06760
ACS Omega 2023, 8, 5506−5521

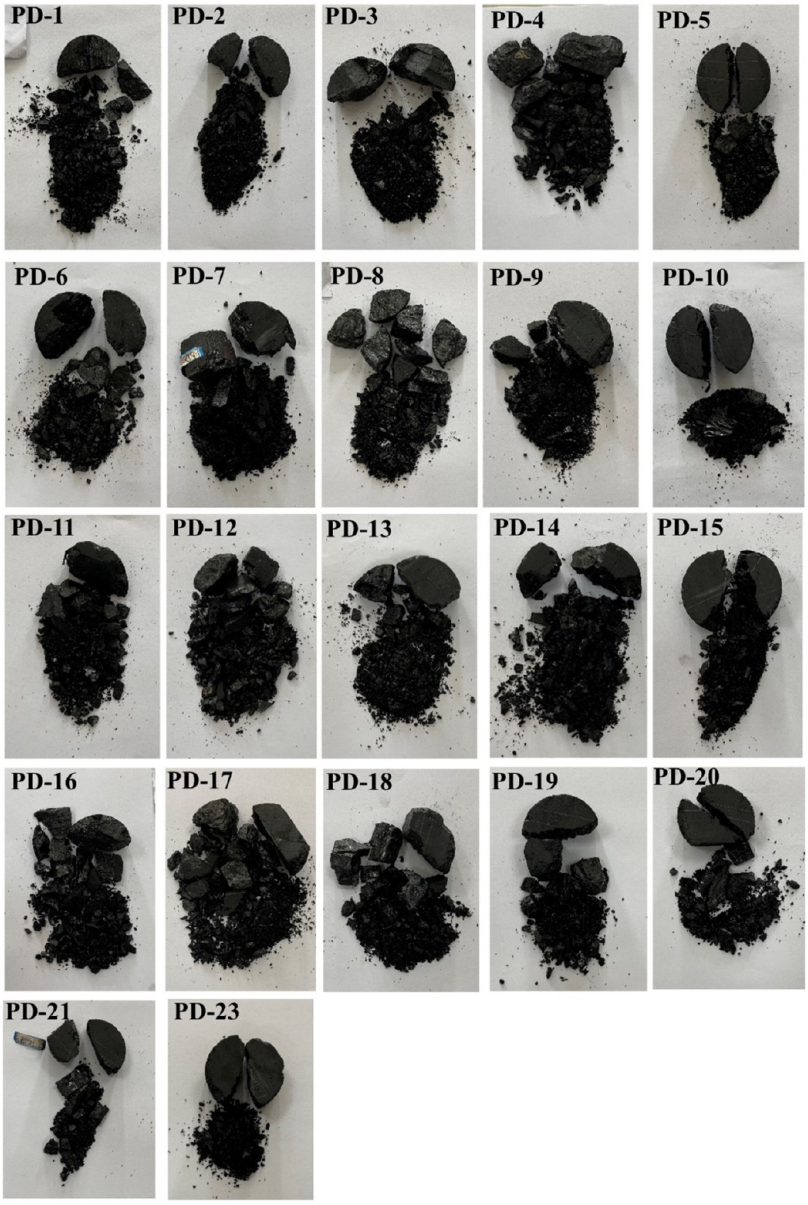

Figure 15. Failure modes of PD group coal samples.

mechanical characteristics of the CD group coal sample during the dynamic tensile test.

According to the resutls shown in Figure 3, when the impact velocity is greater than 4.75 m/s, the average dynamic tensile strength is CD group > PD group coal samples. The maximum strain rate and the impact velocity in the CD and PD group coal samples both show a proportional relationship. However, under the same conditions of the first-order function fitting, the fitting degree between the maximum strain rate and the impact velocity of the CD group is higher than the PD group coal samples. It can be seen that the dynamic deformation modulus of the CD group is greater than that of the PD group coal samples.

Therefore, in terms of the dynamic tensile mechanical properties of coal specimens with the CD group (vertically bedding) are better than the PD group (parallel bedding).

5.2. Effect of the Impact Angle on Tensile Characteristics of Coal Samples. The relationship between tensile strength and impact angle of coal samples in the PD group under different impact angles is shown in Figure 16. When the impact angle is 0°, cracks already appear in the PD-9 and PD-11 coal samples during the test preloading stage. Therefore, the

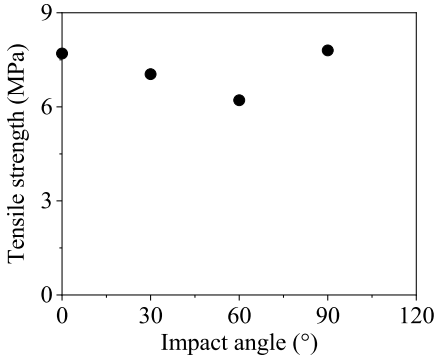

Figure 16. The relationship between the tensile strength and impact angle.

https://doi.org/10.1021/acsomega.2c06760
ACS Omega 2023, 8, 5506−5521

tensile strength data of the PD-9 and PD-11 coal samples show that they do not participate in the statistical regression of the PD group.

From Figure 16, we can find that the impact angle was fitted to the data of the dynamic tensile strength of the coal sample, and the fitting relationship is as follows

$$y = 0.56x^2 - 2.87x + 10.13 \quad R^2 = 0.79 \tag{15}$$

As eq 15 shows, under the conditions of the impact angles of 0, 30, 60, and 90°, the correlation coefficient R^2 value is 0.79. This indicates that the impact angle has a weaker effect on the dynamic tensile strength of the coal sample. There was no obvious relationship between the dynamic tensile strength and impact angle of the PD group coal sample, and it was observed that the dynamic tensile strength of the coal sample was less affected by the impact angle between the impact direction and the coal layer. The minimum average dynamic tensile strength of the PD group coal samples was 6.21 MPa, and the maximum value was 7.80 MPa, corresponding to the impact angles of 60 and 90°, respectively.

6. CONCLUSIONS

In this paper, the dynamic tensile experiment of the coal samples was carried out. The dynamic tensile strength, deformation, and energy evolution characteristics of the coal samples under the SHPB test system were analyzed. According to the experimental results, the following conclusions were drawn:

(1) The dynamic tensile mechanical parameters of the CD group coal samples show a discrete distribution when the dynamic impact velocity is less than 4.75 m/s. When the impact velocity is greater than 4.75 m/s, the dynamic tensile strength, strain, and strain rate values of the CD group coal samples constantly increased. By contrast, the first and second dynamic deformation moduli, and dynamic failure time of coal samples are constantly decreasing. Under the same impact velocity conditions, the dynamic tensile strength of the vertically layered CD group was greater than that of the parallel stratification PD group coal samples.

(2) The dynamic impact angles range from 0 to 90°, and the dynamic tensile strength of the PD group coal specimens was increased. The values of peak strain, ultimate strain, and strain rate of the coal samples are maximum at the impact angle of 0°. The first and second dynamic deformation moduli of the PD group coal samples have the largest values at an impact angle of 30°. In addition, it was noted that impact angle has little influence on the dynamic tensile strength and deformation parameter change of the PD group coal samples.

(3) Based on the monitoring of the failure process of coal samples, it was found that the energy evolution and failure characteristics have similar features. With the increase of incident energy, the sum of reflected energy and transmitted energy was increased, and absorb energy also increased for the CD and PD group coal samples. The failure model was mainly tensile failure, and there was also existing shear failure in the fracture development position of the two types of coal samples. The greater the impact velocity, the more obvious crushing characteristics of coal samples, and the fractal dimension of crushed coal samples increased. Moreover, after the complete failure of coal samples, multiple small coal sample fragments will be formed. The impact angles mainly affect the crack growth characteristics of the PD group coal samples.

AUTHOR INFORMATION

Corresponding Author

Yuzhong Yang − *School of Energy Science and Engineering, Henan Polytechnic University, Jiaozuo, Henan 454000, China;* orcid.org/0000-0003-0040-4518; Email: jityyz@hpu.edu.cn

Authors

Han Meng − *School of Mining and Geomatics Engineering, Hebei University of Engineering, Handan, Hebei 056038, China;* orcid.org/0000-0003-1650-6287

Liyun Wu − *School of Energy Science and Engineering, Henan Polytechnic University, Jiaozuo, Henan 454000, China;* orcid.org/0000-0003-3655-0437

Daming Yang − *School of Mining and Geomatics Engineering, Hebei University of Engineering, Handan, Hebei 056038, China*

Chenlin Wang − *School of Mining and Geomatics Engineering, Hebei University of Engineering, Handan, Hebei 056038, China*

Complete contact information is available at: https://pubs.acs.org/10.1021/acsomega.2c06760

Author Contributions

H.M.: Writing − original draft and investigation. Y.Y.: Writing − review & editing. L.W.: Investigation and writing − original draft. D.Y.: Conceptualization and methodology. C.W. − review & editing and formal analysis.

Notes

The authors declare no competing financial interest.
Data will be made available on request.

ACKNOWLEDGMENTS

This work was supported in part by the National Natural Science Foundation of China under grants (51874121, U1904210, 52104081) and the National Natural Science Foundation of Hebei Province (E2022402031, E2020402041).

REFERENCES

(1) Xie, H. P.; Zhu, J. B.; Zhou, T.; Zhao, J. Novel three-dimensional rock dynamic tests using the true triaxial electromagnetic Hopkinson bar system. *Rock. Mech. Rock. Eng.* **2021**, *54*, 2079−2086.

(2) Lu, S. Q.; Li, M. J.; Ma, Y. K.; Wang, S. C.; Zhao, W. Permeability changes in mining-damaged coal: A review of mathematical models. *J. Nat. Gas. Sci. Eng.* **2022**, *106*, No. 104739.

(3) Li, X. L.; Chen, S. J.; Wang, S.; Zhao, M.; Liu, H. Study on in situ stress distribution law of the deep mine: taking linyi mining area as an example. *Adv. Mater. Sci. Eng.* **2021**, *2021*, 1−11.

(4) Chen, S. D.; Tang, D. Z.; Tao, S.; Liu, P. C.; Mathews, J. P. Implications of the in situ stress distribution for coalbed methane zonation and hydraulic fracturing in multiple seams, western Guizhou, China. *J. Petrol. Sci. Eng.* **2021**, *204*, No. 108755.

(5) Zhang, T. Y.; Tao, S.; Tang, D. Z.; Tang, S. L.; Xu, H.; Zhang, A. B.; Pu, Y. F.; Liu, Y. Y.; Yang, Q. Permeability anisotropy in high dip angle coal seam: A case study of southern junggar basin. *Nat. Resour. Res.* **2021**, *30*, 2273−2286.

(6) Shu, L. Y.; Wang, K.; Liu, Z. S.; Zhao, W.; Zhu, N. N.; Lei, Y. A novel physical model of coal and gas outbursts mechanism: Insights

https://doi.org/10.1021/acsomega.2c06760
ACS Omega 2023, 8, 5506−5521

into the process and initiation criterion of outbursts. *Fuel* **2022**, *323*, No. 124305.
(7) Liu, S. M.; Li, X. L.; Wang, D. K.; Zhang, D. M. Investigations on the mechanism of the microstructural evolution of different coal ranks under liquid nitrogen cold soaking. *Energy. Sources. Part A* **2020**, 1−17.
(8) Liu, H. Y.; Zhang, B. Y.; Li, X. L.; Liu, C. W.; Wang, C.; Wang, F.; Chen, D. Y. Research on roof damage mechanism and control technology of gob-side entry retaining under close distance gob. *Eng. Fail. Anal.* **2022**, *138*, No. 106331.
(9) Wang, S.; Li, X. L.; Qin, Q. Z. Study on surrounding rock control and support stability of ultral-large height mining face. *Energies* **2022**, *15*, 6811.
(10) Li, Q. M.; Meng, H. About the dynamic strength enhancement of concrete-like materials in a split Hopkinson pressure bar test. *Int. J. Solids. Struct.* **2003**, *40*, 343−360.
(11) Li, Q. M.; Reid, S. R.; Wen, H. M.; Telford, A. R. Local impact effects of hard missiles on concrete targets. *Int. J. Impact. Eng.* **2005**, *32*, 224−284.
(12) Zhou, X. Q.; Hao, H. Modelling of compressive behavior of concrete-like materials at high strain rate. *Int. J. Solids Struct.* **2008**, *45*, 4648−4661.
(13) Li, Q. M.; Lu, Y. B.; Meng, H. Further investigation on the dynamic compressive strength enhancement of concrete-like materials based on split Hopkinson pressure bar tests. Part II: Numerical simulations. *Int. J. Impact. Eng.* **2009**, *36*, 1335−1345.
(14) Frew, D. J.; Forrestal, M. J.; Chen, W. A Split Hopkinson pressure bar technique to determine compressive stress-strain data for rock materials. *Exp. Mech.* **2001**, *41*, 40−46.
(15) Hao, Y.; Hao, H. Numerical investigation of the dynamic compressive behavior of rock materials at high strain rate. *Rock. Mech. Rock. Eng.* **2013**, *46*, 373−388.
(16) Qi, P.; Ma, Q. Y.; Yuan, P. Energy dissipation analysis of stone specimens in SHPB tensile test. *J. Min. Saf. Eng.* **2013**, *30*, 401−407.
(17) Xu, Y.; Dai, F. Dynamic response and failure mechanism of brittle rocks under combined compression shear loading experiments. *Rock. Mech. Rock. Eng.* **2018**, *51*, 747−764.
(18) Jiang, F.; Vecchio, K. S. Hopkinson bar loaded fracture experimental technique: A critical review of dynamic fracture toughness tests. *Appl. Mech. Rev.* **2009**, *62*, 060802.
(19) Wang, Q. Z.; Li, W.; Xie, H. P. Dynamic split tensile test of flattened Brazilian disc of rock with SHPB setup. *Mech. Mater.* **2009**, *41*, 252−260.
(20) Li, Q.; Meng, H. About the dynamic strength enhancement of concrete-like materials in a Hopkinson pressure bar test. *Int. J. Solids. Struct.* **2003**, *40*, 343−360.
(21) Kumar, A. The effect of stress rate and temperature on the strength of basalt and granite. *Geophysics* **1968**, *33*, 501−510.
(22) Hakalehto, K. O. The behavior of rock under impulse loads a study using the split Hopkinson Bar method. *Acta. Polytechnica. Scandinavica.* **1969**, 16−49.
(23) Klepaczko, J. R.; Bassim, M. N.; Hsu, T. R. Fracture toughness of coal under quasi-static and impact loading. *Eng. Fract. Mech.* **1984**, *19*, 305−316.
(24) Wang, Q. Z.; Zhang, S.; Xie, H. P. Rock dynamic fracture toughness tested with hole-cracked flattened Brazilian discs diametrically impacted by SHPB and its size effect. *Exp. Mech.* **2010**, *50*, 877−885.
(25) Dai, F.; Huang, S.; Xia, K. W.; Tan, Z. Y. Some fundamental issues in dynamic compression and tension tests of rocks using split Hopkinson pressure bar. *Rock. Mech. Rock. Eng.* **2010**, *43*, 657−666.
(26) Chen, W. W.; Song, B.*Split Hopkinson (Kolsky) Bar: Design, Testing and Applications*, Springer: New York, 2011.
(27) Zhang, Q. B.; Zhao, J. A review of dynamic experimental techniques and mechanical behaviour of rock materials. *Rock. Mech. Rock. Eng.* **2014**, *47*, 1411−1478.
(28) Wang, Q. Z.; Li, W.; Song, X. L. A method for testing dynamic tensile strength and elastic modulus of rock materials using SHPB. *Pure. Appl. Geophys.* **2006**, *163*, 1091−1100.
(29) Ai, D. H.; Zhao, Y. H.; Wang, Q. F.; Li, C. W. Crack propagation and dynamic properties of coal under SHPB impact loading: Experimental investigation and numerical simulation. *Theor. Appl. Fract. Mech.* **2020**, *105*, No. 102393.
(30) Zhao, Y. X.; Gong, S.; Huang, Y. Q. Experimental study on energy dissipation characteristics of coal samples under impact loading. *J. China. Coal. Soci.* **2015**, *40*, 2320−2326.
(31) Zhao, Y. X.; Zhao, G. F.; Jiang, Y. D.; Elsworth, D.; Huang, Y. Q. Effects of bedding on the dynamic indirect tensile strength of coal: Laboratory experiments and numerical simulation. *Int. J. Coal Geol.* **2014**, *132*, 81−93.
(32) Zhang, Q. B.; Zhao, J. Determination of mechanical properties and full-field strain measurements of rock material under dynamic loads. *Int. J. Rock. Mech. Min.* **2013**, *60*, 423−439.
(33) Zhu, X. L.; Li, Q.; Wei, G. H.; Fang, S. Z. Dynamic tensile strength of dry and saturated hard coal under impact loading. *Energies* **2020**, *13*, 1273.
(34) Xia, K. W.; Huang, S.; Jha, A. K. Dynamic tensile test of coal, shale and sandstone using split Hopkinson pressure bar: A tool for blast and impact assessment. *Int. J. Geotech. Earthq.* **2010**, *1*, 24−37.
(35) Gong, F. Q.; Zhao, G. F. Dynamic indirect tensile strength of sandstone under different loading rates. *Rock. Mech. Rock. Eng.* **2014**, *47*, 2271−2278.
(36) Huang, S.; Xia, K. W.; Yan, F.; Feng, X. An experimental study of the rate dependence of tensile strength softening of Longyou sandstone. *Rock. Mech. Rock. Eng.* **2010**, *43*, 677−683.
(37) Lundberg, B. A split Hopkinson bar study of energy absorption in dynamic rock fragmentation. *Int. J. Rock. Mech. Min. Sci. Geomech. Abst.* **1976**, *13*, 187−197.
(38) Zhang, T.; Liu, B.; Wei, Z.; Jiao, Z. H.; Song, Z. Y.; Zhang, H. W. Dynamic mechanical response and crack evolution of burst-prone coal with a single prefabricated fissure. *Theor. Appl. Fract. Mec.* **2022**, *121*, No. 103494.
(39) Li, X. B.; Lok, T. S.; Zhao, J. Dynamic characteristics of granite subjected to intermediate loading rate. *Rock. Mech. Rock. Eng.* **2005**, *38*, 21−38.
(40) Xu, Y.; Dai, F. Dynamic response and failure mechanism of brittle rocks under combined compression shear loading experiments. *Rock. Mech. Rock. Eng.* **2018**, *51*, 747−764.
(41) Zhou, Y. X.; Xia, K.; Li, X. B.; Li, H.; Ma, G. W.; Ma, G.; Zhao, J.; Zhao, J.; Zhou, Z. L.; Zhou, Z.; Dai, F. Suggested methods for determining the dynamic strength parameters and mode-I fracture toughness of rock materials. *Int. J. Rock Mech. Min.* **2012**, *49*, 105−112.
(42) ISRM. The Complete ISRM Suggested Methods for Rock Characterization, Testing and Monitoring: 1974-2006. In *Prepared by the Commission on Testing Methods*, Ulusay, R.; Hudson, J. A., Eds.; ISRM: Ankara, 2007.
(43) Ouchterlony, F.Suggested Methods for Determining the Fracture Toughness of Rock. In *The Complete ISRM Suggested Methods for Rock Characterization, Testing and Monitoring; 1974-2006.*, Ulusay, R.; Houdson, J. A., Eds.; ISRM Turkish National Group: Ankara, Turkey, 2007; pp 2321−2358.
(44) Cai, M.; Kaiser, P. K.; Suorineni, F.; Su, K. A study on the dynamic behaviour of the Meuse/Hate-Marne argillite. *Phys. Chem. Earth.* **2007**, *32*, 907−916.
(45) Gong, F. Q.; Li, X. B.; Zhao, J. Analytical algorithm to estimate tensile modulus in Brazilian disk splitting tests. *Chin. J. Rock Mech. Eng.* **2010**, *29*, 881−891.
(46) Jin, J. F.; Yang, Y.; Liao, Z. X.; Yu, X.; Zhong, Y. L. Effect of dynamic loads and geo-stresses on response characteristics of rocks. *Chin. J. Rock. Mech. Eng.* **2021**, *40*, 1990−2002.
(47) Wang, C.; Cheng, L. P.; Tang, L. Z.; Wang, W.; Liu, T.; Wei, Y. H.; Shen, W. L. Effects of the unloading rate on dynamic characteristic and failure modes of rock under high static loads. *Chin. J. Rock. Mech. Eng.* **2019**, *38*, 217−225.
(48) Li, X. B.; Lok, T. S.; Zhao, J.; Zhao, P. J. Oscillation elimination in the Hopkinson bar apparatus and resultant complete dynamic stress-strain curves bar apparatus and resultant complete dynamic

https://doi.org/10.1021/acsomega.2c06760
ACS Omega 2023, 8, 5506−5521

stress-strain curves for rocks. *Int. J. Rock Mech. Min.* **2000**, *37*, 1055−1060.
(49) Li, L. Y.; Xu, Z. Q.; Xie, H. P.; Ju, Y.; Ma, X.; Han, Z. C. Failure experimental study on energy laws of rock under differential dynamic impact velocities. *J. China. Coal. Soc.* **2011**, *36*, 2008−2011.
(50) Ramesh, K. T.; Narasimhan, S. Finite deformation and the dynamic measurement of radial strains in compression Kolsky bar experiments. *Int. J. Solids. Struct.* **1996**, *33*, 3723−3738.
(51) Jin, F. N.; Jiang, M. R.; Gao, X. L. Defining damage variable based on energy dissipation. *Chin. J. Rock. Mech. Eng.* **2004**, *23*, 1976−1980.
(52) Wang, X. L.; Pan, J. N.; Wang, D. K.; Mou, P. W.; Li, J. X. Fracture variation in high-rank coal induced by hydraulic fracturing using X-ray computer tomography and digital volume correlation. *Int. J. Coal. Geol.* **2022**, *252*, No. 103942.

https://doi.org/10.1021/acsomega.2c06760
ACS Omega 2023, 8, 5506−5521